

# The illustrated life cycle of *Microbotryum* on the host plant *Silene latifolia*

Angela Maria Schäfer, Martin Kemler, Robert Bauer, and Dominik Begerow

**Abstract:** The plant-parasitic genus *Microbotryum* (Pucciniomycotina) has been used as a model for various biological studies, but fundamental aspects of its life history have not been documented in detail. The smut fungus is characterized by a dimorphic life cycle with a haploid saprophytic yeast-like stage and a dikaryotic plant-parasitic stage, which bears the teliospores as dispersal agents. In this study, seedlings and flowers of *Silene latifolia* Poir. (Caryophyllaceae) were inoculated with teliospores or sporidial cells of *Microbotryum lychnidis-dioicae* (DC. ex Liro) G. Deml & Oberw. and the germination of teliospores, the infection process, and the proliferation in the host tissue were documented in vivo using light and electron microscopy. Although germination of the teliospore is crucial for the establishment of *Microbotryum*, basidium development is variable under natural conditions. In flowers, where the amount of nutrients is thought to be high, the fungus propagates as sporidia, and mating of compatible cells takes place only when flowers are withering and nutrients are decreasing. On cotyledons (i.e., nutrient-depleted conditions), conjugation occurs shortly after teliospore germination, often via intrapromycelial mating. After formation of an infectious hypha with an appressorium, the invasion of the host occurs by direct penetration of the epidermis. While the growth in the plant is typically intercellular, long distance proliferation seems mediated through xylem tracheary elements. At the beginning of the vegetation period, fungal cells were found between meristematic shoot host cells, indicating a dormant phase inside the plant. By using different microscopy techniques, many life stages of *Microbotryum* are illustrated for the first time, thereby allowing new interpretations of laboratory data.

**Key words:** *Microbotryum*, basidial development, infection process, electron microscopy, smut.

**Résumé :** Le genre parasite des plantes *Microbotryum* (Pucciniomycotina) a fait l'objet de nombreuses études comme modèle pour diverses questions biologiques, mais les aspects fondamentaux de son cycle vital n'ont pas été documentés en détail. Le champignon du charbon se caractérise par un cycle vital dimorphe avec un stade saprophyte haploïde de forme levure et un stade parasite des plantes dicaryotes, ce dernier portant des télisporas comme agent de dispersion. Dans cette étude, les auteurs ont inoculé des plantules et des fleurs du *Silene latifolia* Poir. (Caryophyllaceae) avec des télisporas ou des cellules sporidiales du *Microbotryum lychnidis-dioicae* (DC. ex Liro) G. Deml & Oberw., et ils ont observé la germination des télisporas, le processus d'infection et la prolifération in vivo dans les tissus de l'hôte à l'aide de la microscopie photonique et électronique. Bien que la germination des télisporas soit cruciale pour l'établissement du *Microbotryum*, le développement de la baside varie sous les conditions naturelles. Dans les fleurs, où l'on croit que la quantité de nutriments abonde, le champignon se propage sous forme de sporidies et le couplage de cellules compatibles ne se fait que lorsque les fleurs flétrissent et les nutriments diminuent. Sur les cotylédons (c.-à-d. condition d'épuisement en nutriments), la conjugaison survient peu de temps après la germination des télisporas, souvent par couplage de mycélium intrapromycélien. Après la formation d'une hyphe d'infection avec appressorium, l'invasion de l'hôte s'effectue par pénétration directe de l'épiderme. Alors que la croissance dans l'hôte demeure typiquement intracellulaire, la prolifération à distance semble s'effectuer via les éléments de trachée du xylème. Au début de la période de végétation, on retrouve les cellules fongiques entre les cellules méristématiques de la tige de l'hôte, indiquant un état de phase dormante dans la plante. En utilisant différentes techniques microscopiques, les auteurs arrivent à illustrer plusieurs stades du cycle de vie des *Microbotryum* pour la première fois ce qui permet de nouvelles interprétations des données de laboratoire.

**Mots-clés :** *Microbotryum*, développement basidial, processus d'infection, microscopie électronique, champignon du charbon.

[Traduit par la Rédaction]

## Introduction

Smut-fungal parasites have fascinated scientists for a long time and, owing to their unique life cycle, they were treated

as a monophyletic group (see Baker 1947; Fischer and Holton 1957). However, detailed morphological, biochemical, and molecular studies support an independent evolution of the smut syndrome at least twice within the Basidiomycota.

Received 17 May 2010. Accepted 29 July 2010. Published on the NRC Research Press Web site at botany.nrc.ca on 28 September 2010.

**A.M. Schäfer,<sup>1</sup> M. Kemler, and D. Begerow.** Ruhr-Universität Bochum, Lehrstuhl für Evolution und Biodiversität der Pflanzen, AG Geobotanik, Universitätsstr. 150 ND 03/175, D-44780 Bochum, Germany.

**R. Bauer.** Eberhard-Karls-Universität Tübingen, Lehrstuhl Organismische Botanik, Auf der Morgenstelle 1, D-72076 Tübingen, Germany.

<sup>1</sup>Corresponding author (e-mail: angela.schaefer@rub.de).

**Fig. 1.** (a–i) Appearance of *Microbotryum lychnidis-dioicae* on its host plant *Silene latifolia*. (a) SEM image of *M. lychnidis-dioicae* teliospores. (b) Part of a pistil of *S. latifolia* with pollen and smut spores which are substantially smaller than pollen grains. (c) Fully open, uninfected male flower of *S. latifolia*. (d) Detail of an uninfected anther of *S. latifolia* with yellowish pollen grains. (e) Infected anthers with sporogenous cells and smut spores. (f) Flower bud of an infected plant shortly before anthesis. The bud appears to burst due to the large numbers of teliospores. (g) Longitudinal section of an infected male flower. Note the vast amount of teliospores and the dark appearance of the whole flower. (h) *Hadena bicruris* (Noctuidae), the most prominent pollinator of *S. latifolia*. (i) Flower of *S. latifolia* infected with *M. lychnidis-dioicae*.

One lineage of smut fungi evolved in the Ustilaginomycotina and the other lineage, the Microbotryales, in the Pucciniomycotina (Begerow et al. 1997; Weiss et al. 2004; Bauer et al. 2006). Within the Microbotryaceae, the genus *Microbotryum* is highest in species numbers and contains only parasites of eudicotyledonous plants (Kemler et al. 2006). One group of *Microbotryum* spp. are the anther smuts of the Caryophyllaceae, and these have been studied in greatest detail. Although there is ongoing debate about host specificity of the anther smuts, molecular phylogenetics supports very high host fidelity of these parasites (Lutz et al. 2005, 2008; LeGac et al. 2007; Refrégier et al. 2008), especially on different species of the model genus *Silene* (Bernasconi et al. 2009).

*Microbotryum lychnidis-dioicae* (DC. ex Liro) G. Deml & Oberw. infecting *Silene latifolia* Poir. or *Silene dioica* (L.) Clairv. has been used as a model organism in many studies on ecology, genetics, and the transmission of sexual diseases (e.g., Alexander and Antonovics 1988; Garber and Ruddat 2002; Granberg et al. 2008). Like other smut fungi, *M. lychnidis-dioicae* is characterized by a diphasic life cycle. In its haploid stage, the fungus proliferates with saprophytic sporidia (i.e., yeast cells), whereas in the dikaryotic stage, biotrophic hyphae grow inside the host. The teliospores of *M. lychnidis-dioicae* are dark violet in colour, with a reticulate ornamentation (Fig. 1a; Vánky 1994) and with a diameter of 6–10 µm, substantially smaller than pollen grains of *S. latifolia* (Fig. 1b). Petals of healthy flowers are bright white (Fig. 1c), and mature anthers in male flowers produce yellow pollen grains (Fig. 1d), while female flowers have elongated white pistils. When *S. latifolia* is infected by *M. lychnidis-dioicae*, teliospores are produced in the anthers (Fig. 1e). Since infected anthers burst before flowers open, dark teliospores can already be observed in flower buds (Fig. 1f). In infected female plants, development of the anthers is initiated and further maturation of the ovaries is inhibited (Uchida et al. 2003, 2005). When the flower opens, vast amounts of teliospores emerge, causing a smutted appearance of the floral organs (Fig. 1g). During pollinator (e.g., *Hadena bicruris*, Noctuidae, Lepidoptera; Fig. 1h; Bopp 2003) visits to both healthy (Fig. 1c) and infected flowers (Fig. 1i), insects transfer pollen grains as well as smut spores (Jennersten 1983). With the germination of the teliospores as phragmobasidia (i.e., promycelia), the saprophytic aspect of the life cycle is initiated with the fungus propagating as sporidia.



Werth (1911) published detailed observations on the inoculation of *S. latifolia* flowers of both sexes with *M. lychnidis-dioicae* teliospores, resulting in flowers produc-

ing infected anthers. In addition, he described the partial appearance of disease symptoms in the year of infection, but infection of the whole plant in the second year. Therefore, a dormant phase within the plant was postulated (Werth 1911; but see also Fischer von Waldheim 1869; Fischer and Holton 1957). However, probably due to technical limitations, no further studies were performed. Only in 1980 did Audran and Batcho (1980) show fungal cells in the intercellular spaces of the apical meristem of infected plants, by using transmission electron microscopy (TEM). They showed the proliferation of sporogenous fungal cells in the anthers, but could not observe specialized interaction structures such as haustoria (Audran and Batcho 1980). Fungal proliferation, together with anther development, was documented by Uchida et al. (2003, 2005) using scanning electron microscopy (SEM) and TEM.

Eventually, the steps between the occurrence of fungal mycelium in the anthers and the emergence of teliospores were well documented. By contrast, details of the infection process and its location remain unknown (Hood and Antonovics 1998). Therefore the objectives of our study were (i) to document the infection process of the fungus on seedlings and in flowers of *Silene latifolia* in detail using electron microscopy, (ii) to identify the location of the infection process, and (iii) to investigate whether the fungus can be found in hibernating plant tissue, which proves it is systemic in the host.

## Materials and methods

The germination of teliospores on seedlings was studied using different *Microbotryum* specimens: *M. lychnidis-dioicae* (DB1056) from *S. latifolia* collected near Camembert, France (2007), and *M. lychnidis-dioicae* (DB1057) from *S. dioica*, collected in Bochum, Germany (2007).

Cultures (mating type a1, CBS11780; mating type a2, CBS11781) for later infection studies were obtained from specimen DB1056, maintained on malt–yeast–peptone agar and identified via sequencing of the ITS-rDNA. Single spore colonies were achieved by dilution streaking, and verified with mating tests on agar plates and PCR amplification of the two mating type receptor genes (Yockteng et al. 2007).

Seeds of *S. latifolia* subsp. *alba* were collected in 2006 near Kiel, Germany. *Silene latifolia* were cultivated in a greenhouse and pollinated by hand. Ripe seeds of single flowers were collected and stored at room temperature.

### Infection of seedlings

Seeds of *Silene latifolia* were surface sterilized with 75% ethanol for 10 min and soaked in sterile water overnight. The seeds were placed on plates with plant growth medium (0.04% Murashige & Skoog basal salt mixture (Sigma–Aldrich, Taufkirchen, Germany), 0.01% Murashige & Skoog vitamin powder (Sigma–Aldrich), 0.6% saccharose, and 1.2% agar) and cultivated at room temperature, until the cotyledons were fully developed (10 d). Depending on their heights, the seedlings were either further grown in Petri dishes or covered plastic boxes. The seedlings were inoculated either with 4  $\mu$ L of teliospores suspended in distilled water containing anionic wetting agents (concentration of spores:  $4 \times 10^6 \cdot \text{mL}^{-1}$ ), or 4  $\mu$ L of cell suspension

(ca. OD 50 at 595 nm) in distilled water containing an equal amount of sporidia from both mating types. After inoculation, the plants were grown for 1 to 16 d at three different temperatures (4, 15, or 23 °C).

### Sample preparation

Samples were either fixed in 4% formaldehyde – 1% glutaraldehyde v/v (4F:1G) in 0.2 mol·L<sup>-1</sup> phosphate buffer (pH 7.2) (modified from McDowell and Trump 1976) for at least 24 h at room temperature, or primarily fixed with 5% formalin – 5% acetic-acid – 90% alcohol v/v (FAA) instead of 4F:1G, and not postfixed with OsO<sub>4</sub> (Fig. 2d). For examination by SEM, samples originally fixed in 4F:1G were post-fixed in buffered 1% OsO<sub>4</sub> for 1 h, washed with deionized water (3  $\times$  10 min), dehydrated in an ascending ethanol series, transferred to formaldehyde–dimethylacetale (FDA) for 24 h (Gersterberger and Leins 1978), critical-point dried, and sputter coated with gold for 220 s. The material was examined with a DSM 950 (Zeiss, Oberkochen, Germany) at 15 kV and the results were documented using Digital Image Processing Software 2.2 (DIPS, Leipzig, Germany).

For examination by TEM, the protocol followed the methods of Bauer et al. (1997). Semi-thin sections were stained with new fuchsine – crystal violet and documented using an Olympus BX 51 light microscope and the cell<sup>^</sup>F-software (Olympus, Japan).

### Infection of flowers

*Silene latifolia* plants were cultivated in a greenhouse. In the late afternoon, shortly before the flowers were fully opened, teliospores of *M. lychnidis-dioicae* were placed into the flowers using a toothpick. Simultaneously, female flowers were pollinated with pollen of *S. latifolia*. To avoid disturbance by insects, inoculated plants were covered with a gauze net. Male flowers were collected as soon as they started to drop from the plant (between 1 and 3 days post infection (dpi)). Female flowers were collected at the latest 6 dpi. The collected flowers were fixed with 4% formaldehyde – 1% glutaraldehyde in 0.2 mol·L<sup>-1</sup> phosphate buffer for at least 24 h, washed with buffer (3  $\times$  10 min) and dissected. The following preparation steps were according to the proceedings of the seedlings, except for the post-fixation with OsO<sub>4</sub>.

### Rootstock material

At the beginning of February, parts of rootstocks from *S. latifolia* plants that had shown infection symptoms in the previous year were dug out. The scions of the rootstocks with the first visible green tissue were cut into small pieces, processed according to the protocol for the seedlings, and examined under TEM.

## Results

### Germination of teliospores on seedlings and in flowers

The germination structures of *Microbotryum* teliospores on *S. latifolia* seedlings were identical, irrespective of their different origin (i.e., from *S. latifolia* or *S. dioica*). Thus, we discuss and illustrate our results based on the experiments with spores derived from *S. latifolia*, except when

there was a significant difference in the quality of the pictures.

When seedlings or flowers of *S. latifolia* were inoculated with teliospores, most of the spores had already germinated by the time of harvest (Fig. 2a). Often, fully developed phragmobasidia had detached from the teliospore (Fig. 2e; compare Ingold 1983). During germination, the basidia of *M. lychnidis-dioicae* divided by one or two septa. Only three-celled basidia were observed in flowers (Figs. 2b, 2c), whereas on seedlings most basidia were two-celled (Figs. 2d–2f) with only a proximal and a distal cell. Rather than producing basidiospores, in two-celled basidia, a conjugation hypha was often formed between the proximal and the distal cell (Figs. 2e and 2f). Afterwards, formation of an infectious hypha with a subsequent swollen appressorial structure at the tip of the hypha could be observed (Fig. 2g). In three-celled basidia, each basidial compartment budded off a single basidiospore, while a fourth basidiospore always emerged from the teliospore (Figs. 2b and 2c). Basidiospores reproduced via budding, and the haploid sporidia colonized large parts of the substrate (Fig. 2h). In flowers, teliospores, as well as sporidial cells, were found on petals, pistils (e.g., Fig. 2i), and stamens. Teliospores were absent on the inside of the sepals, which could be due to the inoculation with a toothpick. The same distribution of teliospores was observed in flowers accidentally visited by insect pollinators, which could be easily identified by butterfly scales on pistils (data not shown). Further fungal development (i.e., 3–6 dpi) could only be studied in female flowers, as male flowers of *S. latifolia* stayed open only 1–2 d, which is a much shorter time than female flowers (Shykoff et al. 1996). In contrast to female flowers, where at least the ovary is long lasting, decomposition of the male flower started right after closing.

### Conjugation and infection

The budding sites of the sporidia exhibited typical basidiomycetous scars (Fig. 3a). Conjugation took place between compatible cells, and contact zones of conjugation tubes were clearly visible in early stages of conjugation (Fig. 3b). At later stages of the conjugation, cell walls of the contact zone dissolved to allow the transfer of nuclei (Fig. 3c) and the common tube elongated (Fig. 3d). Sometimes triple conjugations occurred, either by fusion of a third sporidial cell to an already conjugated sporidium (Fig. 3e) or fusion of three conjugation tubes (Fig. 3f). After conjugation, an infectious hypha emerged enteroblastically from one of the conjugated sporidia, producing a collar (Fig. 3g) resembling scars of budding sporidial cells (Fig. 3a). The infectious hyphae were of various lengths and could reach up to 20  $\mu\text{m}$ . In the majority of cases the hyphae grew towards the junctions of anticlinal walls of epidermal cells (Fig. 3h). Infectious hyphae were usually short when conjugation had already occurred in this area (Fig. 3i). Sometimes, development of infection structures could not be connected to these plant structures (Fig. 4a).

Prior to penetration of the host surface, swollen appressoria occurred at the end of the infectious hyphae (Fig. 4b). At the lower part of appressoria, the fungal cell wall was in close contact with the host epidermis (Fig. 4c). After successful penetration of the host epidermis, the fungal cyto-

plasm was retracted and evacuated infectious hyphae collapsed (Fig. 4d). At this stage, septae for sealing off infectious hyphae were clearly visible (Fig. 4e).

Appressoria and collapsed infectious hyphae could be found after 48 h on seedlings inoculated with sporidia, regardless of whether they were cultivated at room temperature (22 °C) or at 15 °C. Following inoculation with teliospores, infection structures were found only after 73 h at room temperature, and no infection structures were observed at 15 °C for up to 9 d. In addition, no infection structures were observed when the seedlings were kept at 4 °C, irrespective of the use of teliospores or sporidia for inoculation.

### In planta growth and systemic infection

After the fungus had successfully entered seedlings of *S. latifolia*, hyphal cells were observed in the intercellular spaces of the host tissue (Fig. 4f) and in the xylem tracheary elements (Figs. 4g, 4h). Fungal cells could be observed (Figs. 5a–5c) between apical meristematic cells of scions derived from rootstocks of infected and dormant plants. Also, at the surface of shoots, sporidia-like cells could sometimes be found (Figs. 5d, 5e). Inside the plant tissue of the same sample, hyphal cells with electron-transparent cell walls were observed (Figs. 5e, 5f). Because of the electron-transparent cell walls, these cells were interpreted as very young stages of *M. lychnidis-dioicae* shortly after the infection of the host plant.

### Discussion

In our study, important steps of the life cycle of *M. lychnidis-dioicae* are visualized by the use of electron microscopy for the first time. On the basis of our observations, it is possible to link results from laboratory experiments with more natural conditions, thereby closing gaps in the understanding of the life history of *Microbotryum*.

### Germination of teliospores on seedlings and in flowers

Previous studies demonstrated that the number of basidial cells produced by *Microbotryum* is dependent on nutrient availability and temperature. When kept under low nutrient and low temperature conditions, *Microbotryum* mainly produces two-celled basidia, while mainly three-celled basidia are produced when kept in richer nutrient and higher temperature conditions (Huettig 1931; Hood and Antonovics 1998). These conditions were assumed to be general stress factors, but differences in basidia formation could not be correlated to natural conditions of the *Microbotryum–Silene* interaction (Hood and Antonovics 1998). In our microscopy study, two-celled basidia could only be observed on the epidermis of *Silene* seedlings. Although we do not know the amount of sugar on the surface of *Silene* seedlings, leaf surfaces of different mature plant species have generally low sugar contents, between  $0.06 \pm 0.02 \mu\text{g}$  and  $1.55 \pm 0.38 \mu\text{g}$  per gram of leaf (Mercier and Lindow 2000). In two-celled basidia, the segregation of nuclei in the distal cell from the second meiotic division is not followed by a segmentation event, and the distal cell remains bikaryotic, whereas the proximal cells become monokaryotic, owing to the migration of the second nucleus back into the teliospore (Hood

**Fig. 2.** (a–i) Germination of teliospores and proliferation of *Microbotryum* in flowers and on seedlings of *Silene latifolia* as viewed with SEM. (a) The germination of fresh teliospores in a flower of *S. latifolia*. (b) Germinated teliospores on petals. Two septa are visible in the phragmobasidia (arrowheads). Three basidiospores are coming out of the basidium (black arrows) while a fourth basidiospore is emerging from the teliospore (white arrow). (c) Detailed view of a germinated teliospore on a petal of *S. latifolia*. Numbers indicate the nomenclature of a phragmobasidium after the second meiotic division referred to in the discussion. I, proximal cell; II, middle cell; III, distal cell. Arrowhead points to a fourth basidiospore, which is emerging from the teliospore. (d) On the seedling surface, in many cases only one septum has formed in the basidium (arrows) because after the second meiotic division, the cell wall between the distal nuclei is not formed. In this case, intrapromycelial conjugation often occurs (arrowheads). Sample is fixed with FAA; therefore, the shrinking is more prominent. (e) Detailed view of phragmobasidia with one septum (arrow) and intrapromycelial conjugation (arrowhead). (f) Because of the shrinking due to chemical fixation, the septum division of the basidium is clearly visible (arrow). The two cells of the basidium are only kept together by the hyphal part needed for intrapromycelial conjugation (arrowhead). (g) When intrapromycelial mating occurs (arrowhead), the infectious hypha with the subsequent appressorium is formed from the basidium (note: *M. lychnidis-dioicae* from *S. dioica* on seedling of *S. latifolia*). (h) Basidia and sporidial cells in the nectar of a *S. latifolia* flower. The polysaccharides of the nectar form a net-like structure, owing to chemical fixation. In the presence of nutrients, the original basidiospores propagate vegetatively via budding (arrowheads). (i) Infection structures at the base of the pistil in a female flower of *S. latifolia* (arrowheads) 4 days post infection.

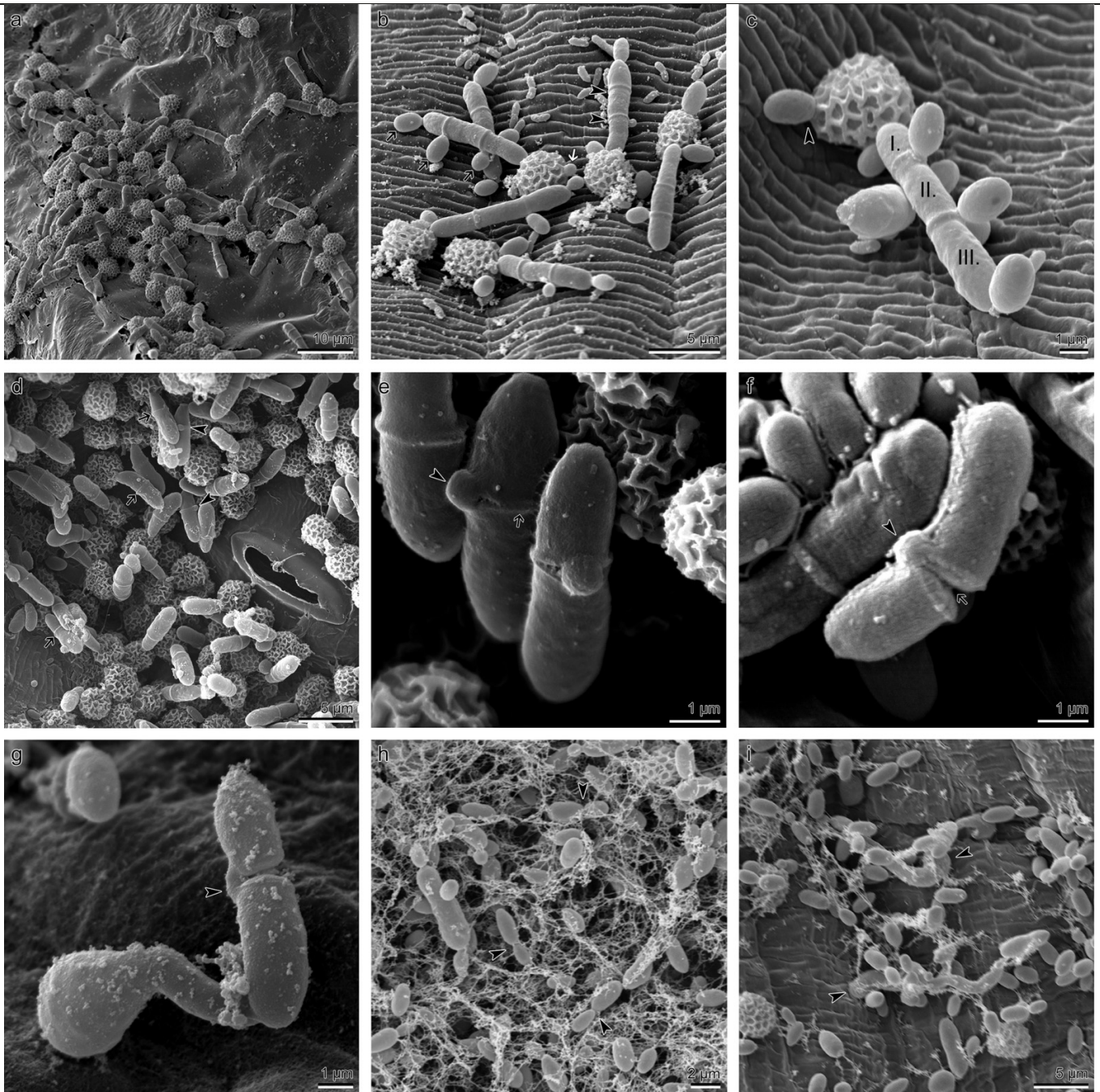
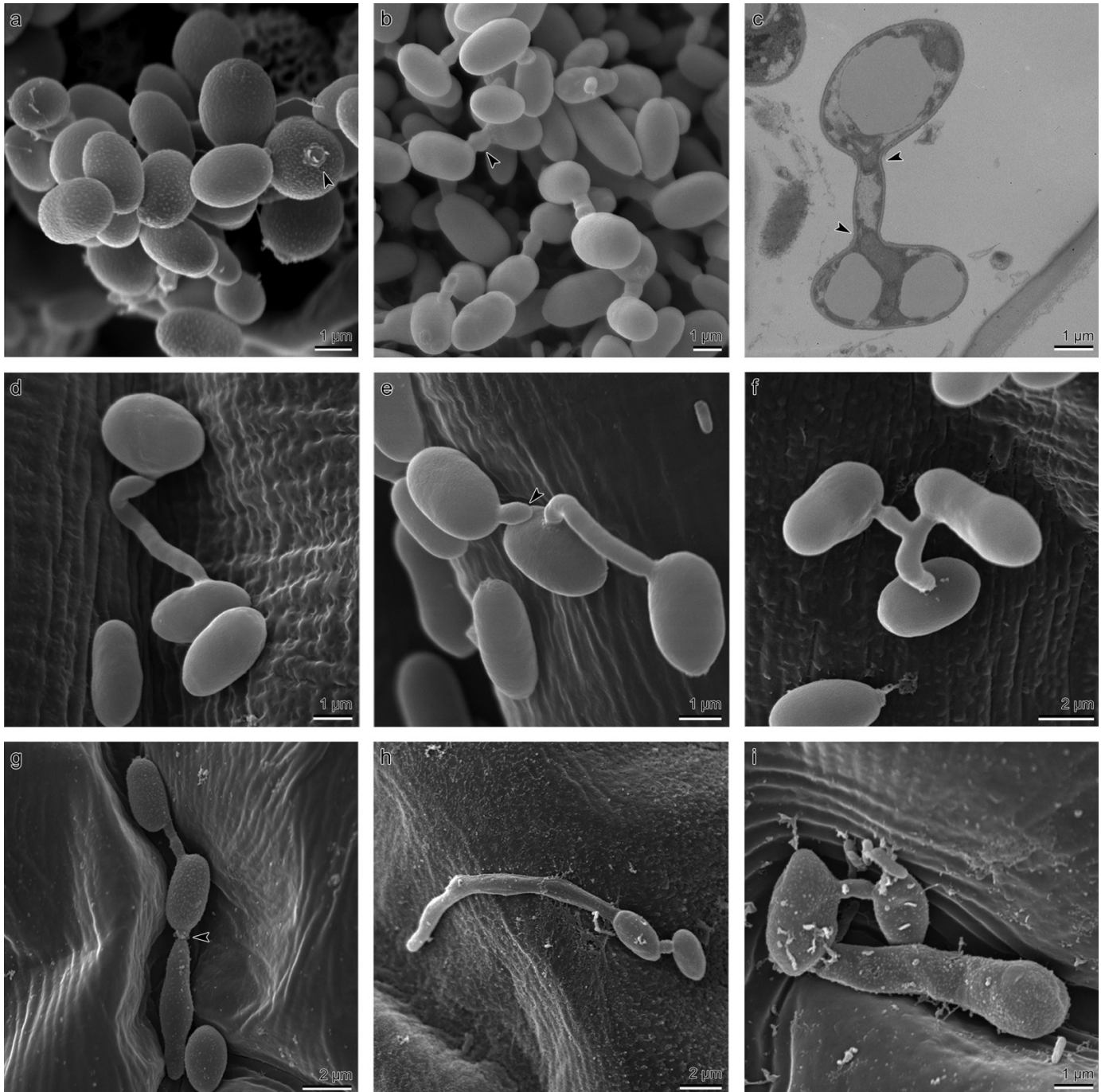


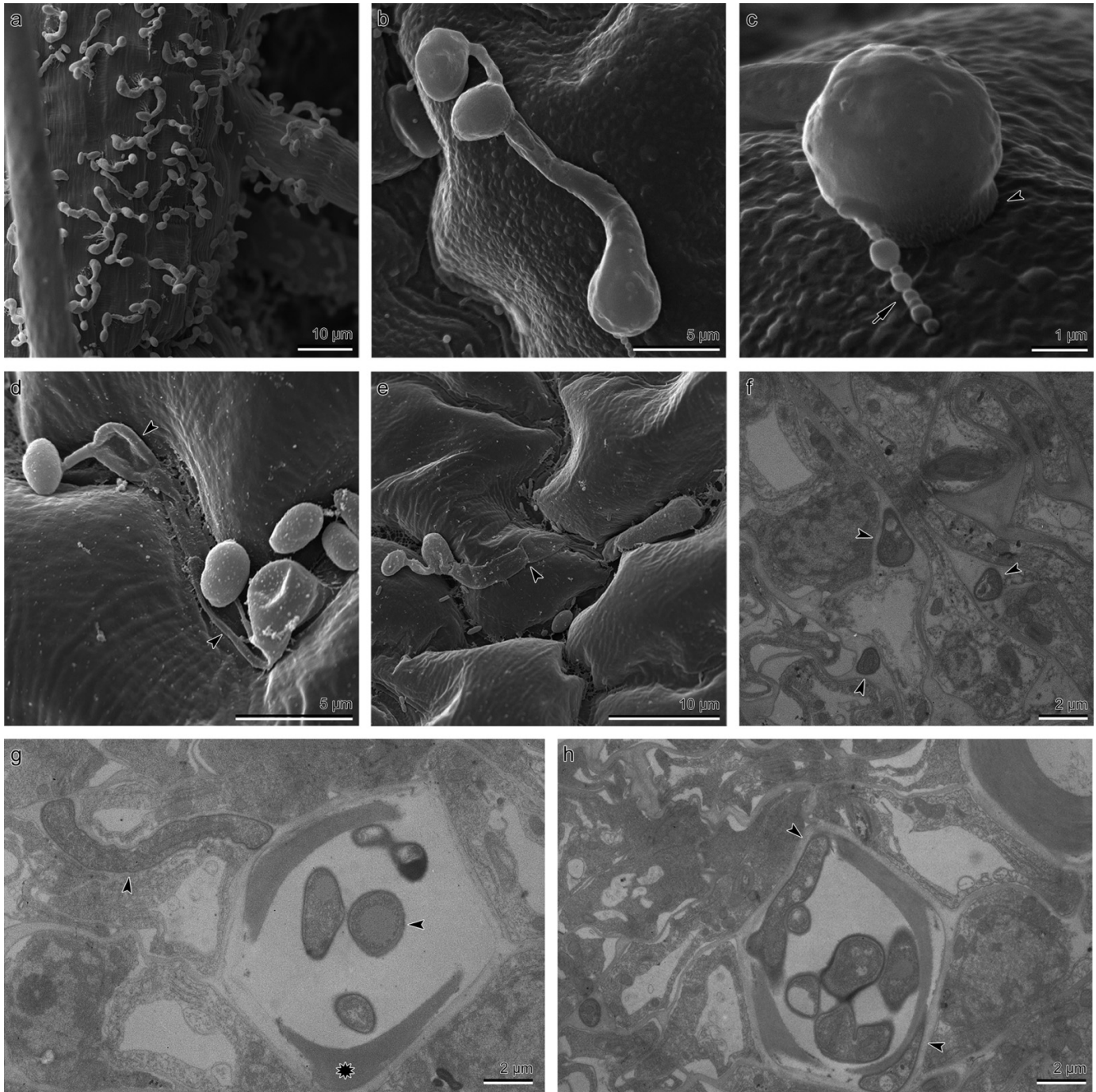
**Fig. 3.** (a–i) Conjugation of cells of different mating type and development of infectious hyphae on the surface of seedlings of *S. latifolia* viewed with SEM (Figs. 3a, 3b, 3d–3i) and TEM (Fig. 3c). (a) Detail view of sporidia. The typical basidiomycetous scar (arrowhead) is visible at the location of former budding. (b) Early stage of conjugation of sporidia of different mating types. The contact zone (arrowhead) is clearly visible. (c) Section of an early stage of conjugation. The cell wall is fully dissolved but the nuclei (arrowheads) are not yet transferred. (d) Older stage of conjugation. The conjugation tube has elongated. (e) A third sporidial cell (arrowhead) is in contact with a conjugated sporidial pair. (f) Triple conjugation between sporidia. (g) At the early stage, the infectious hypha has almost the same diameter as the sporidia. At the beginning of the infectious hypha, the disruption of the original fungal cell wall is visible as a collar (arrowhead). (h) The diameter of the infectious hypha is becoming smaller, while it is elongating to reach the junction of anticlinal plant cell walls, where the swelling of an appressorium will take place. (i) When the conjugated sporidia are in the junction between two epidermal cells, the infectious hypha is very short.



and Antonovics 1998). As the two nuclei in the distal cell are of the same mating type, formation of infection structures can only be obtained through fusion with a cell of the

other mating type. Under conditions with low nutrients and low temperatures, the conjugation between cells of the same basidium on artificial medium was promoted by fusion of

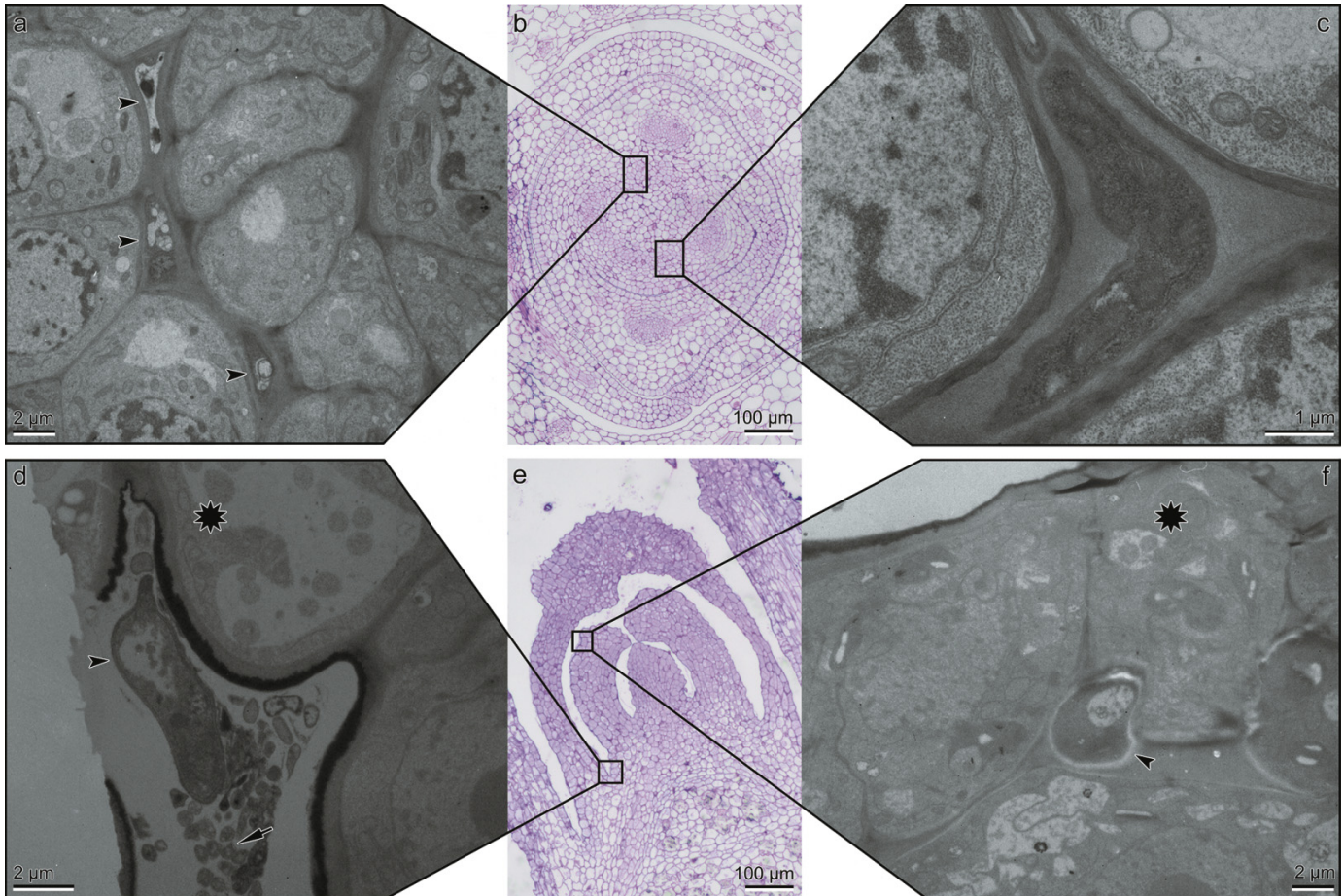
**Fig. 4.** (a–h) Infection structures of *Microbotryum lychnidis-dioicae* on seedlings and proliferation in tissue of *Silene latifolia* viewed with SEM (Figs. 4a–4d) and TEM (Figs. 4f–4h). (a) Sometimes a mass production of infection structures can be seen, where the growing of infectious hyphae are not directed to any plant structure. (b) Before penetration of the host epidermis takes place, the tip of the infectious hypha swells, forming an appressorium. (c) At the edge of the appressorium, no rim of fibrous material is visible (arrowhead). (The chain-like structure (arrow) is an accumulation of organic material due to chemical fixation.) (d) During the invasion of the fungus in the host tissue, its cytoplasm is retracted and the remaining evacuated infectious hypha has collapsed (arrowheads). (e) In the collapsed infectious hypha a septum is visible (arrowhead). (f) In the plant, fungal cells can be seen in the intercellular space (arrowheads). The sample was fixed 8 days post infection. (g) In the same sample, the fungus (arrowhead) is close to tracheary elements of the xylem of its host plant, and fungal cells (arrowhead) can be observed in a tracheary element (identified by the spiral thickenings, star). (h) The fungus is firmly attached to the wall of a tracheary element (arrowheads), growing between the spiral thickenings.



the monokaryotic proximal cell with the bikaryotic distal cell (Hood and Antonovics 1998) and our study confirms that this is also prevalent in vivo (Figs. 2e, 2f). By contrast,

the triple-celled basidia were mainly observed in the flowers of *S. latifolia*, where nectar volumes of up to 3  $\mu\text{L}$  per flower, with a glucose/fructose concentration of 700  $\mu\text{g}\cdot\mu\text{L}^{-1}$ ,

**Fig. 5.** (a–f) Images of tissue sections of dormant *Silene latifolia* rootstocks viewed with TEM (Figs. 5a, 5c, 5d, 5f) and light microscopy (Figs. 5b, 5e). (a) Fungal cells (arrowheads) between meristematic cells of *S. latifolia*. (b) Semi-thin cross section of an apex of an early shoot of *S. latifolia*, origin of the ultra-thin sections of Figs. 5a + 5c. (c) Cell of *M. lychnidis-dioicae* in the intercellular space. (d) Fungal cell (arrowhead) on the surface of a rootstock of a dormant plant. The small cells (arrow) are bacteria. Star indicates the epidermal cell of the plant. (e) Semi-thin longitudinal section of an apex of an early shoot of *S. latifolia*, origin of the ultra-thin sections of Figs. 5d + 5f. (f) Fungal cell (arrowhead) found between plant cells of the same sample. Because of the electron-transparent cell wall, a very young stage of the smut fungus is assumed. Star indicates the epidermal cell of the plant.



were detected (Witt et al. 1999). The triple-celled basidia in our study produced sporidia (Figs. 2b and 2c), while conjugation events between cells within the same promycelium were not observed. As long as the flowers were producing nectar, the fungus was readily proliferating via budding. Fusion between sporidia and the production of infection structures were visible only when flowers started to wither (i.e., 4 dpi in female flowers), which confirms data showing the initiation of conjugation caused by low nutrient levels (Day and Garber 1988). Since the amount of sporidia is positively correlated with infection success (Kaltz and Shykoff 1999), we assume that the saprophytic part of the life cycle of *Microbotryum* serves to increase the amount of cells for a higher infection success on the host plant.

### Conjugation and infection

Conjugation between sporidia of different mating types normally occurs only between cells within close proximity (Poon et al. 1974), and first contact of the cells is aided by microtubules, followed by the establishment of pegs. Finally, a conjugation tube is formed (Poon et al. 1974). In

our study, microtubules were not visible. In rare circumstances, the development of a tube (i.e., peg; mating hypha) out of a solitary sporidial cell was observed (data not shown) on the seedling surface; this reached a length up to 6  $\mu\text{m}$ , which is longer than observed on artificial media (Poon et al. 1974). Long distance growth of mating hyphae to reach a compatible partner, such as occurs in *Ustilago maydis*, was never observed (Snetselaar and Mims 1992).

In our study, infectious hyphae of *M. lychnidis-dioicae* always originated from one of the mated cells, while in *U. maydis*, they either grow out of one of the mated cells or the middle of the conjugation tube (Snetselaar and Mims 1993). Whether this behaviour reflects differences among Microbotryales and Ustilaginomycotina in the transfer of nuclei between conjugated sporidia will have to be investigated in future studies. In contrast to rust fungi, which often use a topographical signal of the epidermis for appressoria development (Allen et al. 1991), we could not identify epidermal structures essential for infection (Figs. 4a and 4b). However, it seemed that the junction of anticlinal epidermis cells was preferred for appressoria development (Figs. 3h, 3i, and 4e).

*M. lychnidis-dioicae* never invaded its host through stomata, and therefore the location of penetration was similar to other smut fungi (Snetselaar and Mims 1993) but different from the dikaryotic mycelium of rust fungi (Heath 1995).

At the beginning of the penetration process, the tip of the infectious hypha swelled to form an appressorium. In *U. maydis*, a rim of fibrous material around the appressorium was observed (Snetselaar and Mims 1993); we were unable to detect similar structures for *M. lychnidis-dioicae* (Fig. 4c). Thus, the adhesion of the fungus might be mediated through proteins or carbohydrates, as found for other plant parasites (Mendgen et al. 1996). According to Mendgen et al. (1996), a fully developed appressorium is characterized by the presence of a septum separating the appressorium from the infectious hypha, allowing the development of high pressure to penetrate the host cell wall. Penetration using high pressure could be shown for *Magnaporthe grisea* after full development of appressoria (Howard et al. 1991). Since we could not detect septa near the appressoria in *M. lychnidis-dioicae*, we assume that the penetration of the host surface is not mediated by turgor pressure, but more probably by lytic enzymes (compare Brefort et al. 2009). This is supported by the genomic data of *M. lychnidis-dioicae*, which contains sequences coding for lytic enzymes similar to those of *U. maydis* (Kämper et al. 2006; Yockteng et al. 2007). After penetration of the host epidermis, the fungal cytoplasm was retracted and empty parts of the infectious hyphae finally collapsed (Figs. 4d and 4e).

### In planta growth and systemic infection

In contrast to *U. maydis* and other members of the Ustilaginales, which grow inter- and intracellularly (Snetselaar and Mims 1992, 1993), *Microbotryum* is reported to grow exclusively intercellularly (Fig. 4f; Bauer et al. 1997). Our study showed *Microbotryum* inside xylem tracheary elements for the first time (Figs. 4g and 4h). Therefore, we assume that long-distance growth from the infection site to shoot meristems is mediated via the continuum of dead cells of the xylem, thus enabling rapid distribution of the fungus within the plant. Nevertheless, no structural interaction with the host plant was observed; therefore, it is still unclear how the fungus gets nutrients from the host (Bauer et al. 1997).

Beside the proliferation of the fungus in planta in the first year, the persistence of the fungus in perennial plants during unfavourable seasons was unclear. Although field observations suggested systemic infection of *Microbotryum*, fungal cells have never been demonstrated in the dormant tissues of perennial plants (Werth 1911; Fischer and Holton 1957; Alexander and Antonovics 1988). The presence of fungal cells in the rootstock of plants in February (Figs. 5a–5c) supported the long-standing hypothesis of systemic infection. In conclusion, we assume that the fungus is not only growing from the infection site into the meristematic tissue, but also into the root tissue. However, we were not able to demonstrate bidirectional growth in the xylem, but if flower shoots with disease symptoms are cut off in the year of infection, a systemic manifestation of the fungus is inhibited and no infection symptoms appeared in the subsequent vegetation period (Alexander and Antonovics 1988). Additionally, our study indicates that *Microbotryum* was able to infect the rootstock in early spring (Figs. 5d–5f). Therefore,

in the second year, it is not possible to distinguish between systemic infections and new infections of the rootstock based on flower disease symptoms alone.

The evidence in our study strongly indicates that nutrient availability has a lasting effect on the germination process of teliospores, not only in vitro but also in vivo, and therefore is an important aspect in the disease ecology of *Microbotryum*. Overall, the detailed illustrations of the life cycle, including the intracellular propagation and the dormant phase in the rootstock, should be of value for future research on host specificity, fungus–plant interactions, and molecular physiology of the model organism *Microbotryum lychnidis-dioicae*.

### Acknowledgements

Special thanks go to M. Wagner-Eha for excellent assistance with the ultra-thin sections and TEM preparation; T. Stützel and S. Adler for assistance at the SEM; E. Schlabs for taking care of the plants; C. Hanschke for overall support; and W. Webster for help with the language. We appreciate the helpful comments of two anonymous reviewers. This research was supported by the German Science Foundation (BE 2201/7-2) and Ruhr-Universität Bochum.

### References

- Alexander, H.M., and Antonovics, J. 1988. Disease spread and population dynamics of anther-smut infection of *Silene alba* caused by the fungus *Ustilago violacea*. *J. Ecol.* **76**(1): 91–104. doi:10.2307/2260456.
- Allen, E.A., Hazen, B.E., Hoch, H.C., Kwon, Y., Leinhos, G.M.E., Staples, R.C., Stumpf, M.A., and Terhune, B.T. 1991. Appressorium formation in response to topographical signals by 27 rust species. *Phytopathology*, **81**(3): 323–331. doi:10.1094/Phyto-81-323.
- Audran, J.C., and Batcho, M. 1980. Aspects infrastructuraux des altérations des anthères de *Silene dioica* parasitées par *Ustilago violacea*. *Can. J. Bot.* **58**(4): 405–415.
- Baker, H.G. 1947. Infection of species of *Melandrium* by *Ustilago violacea* (Pers.) Fuckel and the transmission of the resultant disease. *Ann. Bot. (Lond.)*, **11**: 333–348.
- Bauer, R., Oberwinkler, F., and Vánky, K. 1997. Ultrastructural markers and systematics in smut fungi and allied taxa. *Can. J. Bot.* **75**(8): 1273–1314. doi:10.1139/b97-842.
- Bauer, R., Begerow, D., Sampaio, J.P., Weiß, M., and Oberwinkler, F. 2006. The simple-septate basidiomycetes: a synopsis. *Mycol. Prog.* **5**(1): 41–66. doi:10.1007/s11557-006-0502-0.
- Begerow, D., Bauer, R., and Oberwinkler, F. 1997. Phylogenetic studies on nuclear large subunit ribosomal DNA sequences of smut fungi and related taxa. *Can. J. Bot.* **75**: 2045–2056. doi:10.1139/b97-916.
- Bernasconi, G., Antonovics, J., Biere, A., Charlesworth, D., Delph, L.F., Filatov, D., Giraud, T., Hood, M.E., Marais, G.A.B., McCauley, D., Pannell, J.R., Shykoff, J.A., Vyskot, B., Wolfe, L.M., and Widmer, A. 2009. *Silene* as a model system in ecology and evolution. *Heredity*, **103**(1): 5–14. doi:10.1038/hdy.2009.34. PMID:19367316.
- Bopp, S. 2003. Parasitismus oder Symbiose? Beziehungen zwischen einem parasitischen Bestäuber (*Hadena bicruris* Hufn., Lepidoptera: Noctuidae) und seinen Wirtspflanzen (*Silene*-Arten, Caryophyllaceae). *Zoologica*, No. 152. E. Schweizerbart'sche Verlagsbuchhandlung, Stuttgart, Germany.

- Brefort, T., Doehlemann, G., Mendoza-Mendoza, A., Reissmann, S., Djamei, A., and Kahmann, R. 2009. *Ustilago maydis* as a pathogen. *Annu. Rev. Phytopathol.* **47**(1): 423–445. doi:10.1146/annurev-phyto-080508-081923. PMID:19400641.
- Day, A.W., and Garber, E.D. 1988. *Ustilago violacea*, anther smut of the Caryophyllaceae. *Adv. Plant Pathol.* **6**: 457–482.
- Fischer, G.W., and Holton, C.S. 1957. *Biology and control of the smut fungi.* The Ronald Press Company, New York, N.Y.
- Fischer von Waldheim, A. 1869. Beiträge zur biologie und Entwicklungsgeschichte der Ustilagineen. *Jahrbuch für wissenschaftliche Botanik*, **7**: 61–144.
- Garber, E.D., and Ruddat, M. 2002. Transmission genetics of *Microbotryum violaceum* (*Ustilago violacea*): a case history. *Adv. Appl. Microbiol.* **51**: 107–127. doi:10.1016/S0065-2164(02)51003-0. PMID:12236055.
- Gersterberger, P., and Leins, P. 1978. Rasterelektronenmikroskopische untersuchungen an Blütenknospen von *Physalis philadelphica* (Solanaceae). *Ber. Dtsch. Bot. Ges.* **91**: 381–387.
- Granberg, A., Carlsson-Granér, U., Arnqvist, P., and Giles, B.E. 2008. Variation in breeding system traits within and among populations of *Microbotryum violaceum* on *Silene dioica*. *Int. J. Plant Sci.* **169**(2): 293–303. doi:10.1086/523964.
- Heath, M.C. 1995. Signal exchange between higher plants and rust fungi. *Can. J. Bot.* **73**(S1): 616–623. doi:10.1139/b95-303.
- Hood, M.E., and Antonovics, J. 1998. Two-celled promycelia and mating-type segregation in *Ustilago violacea* (*Microbotryum violaceum*). *Int. J. Plant Sci.* **159**(2): 199–205. doi:10.1086/297539.
- Howard, R.J., Ferrari, M.A., Roach, D.H., and Money, N.P. 1991. Penetration of hard substrates by a fungus employing enormous turgor pressures. *Proc. Natl. Acad. Sci. U.S.A.* **88**(24): 11281–11284. doi:10.1073/pnas.88.24.11281. PMID:1837147.
- Huettig, W. 1931. Über den einfluß der temperatur auf die keimung und geschlechterverteilung bei brandpilzen. *Z. BOT.* **24**: 529–577.
- Ingold, C.T. 1983. The basidium in *Ustilago*. *Trans. Br. Mycol. Soc.* **81**(3): 573–584. doi:10.1016/S0007-1536(83)80128-4.
- Jennersten, O. 1983. Butterfly visitors as vectors of *Ustilago violacea* spores between caryophyllaceous plants. *Oikos*, **40**(1): 125–130. doi:10.2307/3544207.
- Kaltz, O., and Shykoff, J.A. 1999. Selfing versus outcrossing propensity of the fungal pathogen *Microbotryum violaceum* across *Silene latifolia* host plants. *J. Evol. Biol.* **12**(2): 340–349. doi:10.1046/j.1420-9101.1999.00014.x.
- Kämper, J., Kahmann, R., Bölker, M., Ma, L.J., Brefort, T., Saville, B.J., Banuett, F., Kronstad, J.W., Gold, S.E., Müller, O., Perlin, M.H., Wösten, H.A., de Vries, R., Ruiz-Herrera, J., Reynaga-Peña, C.G., Snetselaar, K., McCann, M., Pérez-Martín, J., Feldbrügge, M., Basse, C.W., Steinberg, G., Ibeas, J.I., Holloman, W., Guzman, P., Farman, M., Stajich, J.E., Sentandreu, R., González-Prieto, J.M., Kennell, J.C., Molina, L., Schirawski, J., Mendoza-Mendoza, A., Greilinger, D., Münch, K., Rössel, N., Scherer, M., Vranes, M., Ladendorf, O., Vincon, V., Fuchs, U., Sandroock, B., Meng, S., Ho, E.C., Cahill, M.J., Boyce, K.J., Klose, J., Klosterman, S.J., Deelstra, H.J., Ortiz-Castellanos, L., Li, W., Sanchez-Alonso, P., Schreier, P.H., Häuser-Hahn, I., Vaupel, M., Koopmann, E., Friedrich, G., Voss, H., Schlüter, T., Margolis, J., Platt, D., Swimmer, C., Gnirke, A., Chen, F., Vysotskaia, V., Mannhaupt, G., Güldener, U., Münsterkötter, M., Haase, D., Oesterheld, M., Mewes, H.W., Mauceli, E.W., DeCaprio, D., Wade, C.M., Butler, J., Young, S., Jaffe, D.B., Calvo, S., Nusbaum, C., Galagan, J., and Birren, B.W. 2006. Insights from the genome of the biotrophic fungal plant pathogen *Ustilago maydis*. *Nature*, **444**(7115): 97–101. doi:10.1038/nature05248. PMID:17080091.
- Kemler, M., Göker, M., Oberwinkler, F., and Begerow, D. 2006. Implications of molecular characters for the phylogeny of the Microbotryaceae (Basidiomycota: Urediniomycetes) [online]. *BMC Evol. Biol.* **6**(1): 35 doi:10.1186/1471-2148-6-35. PMID:16638136.
- Le Gac, M., Hood, M.E., Fournier, E., and Giraud, T. 2007. Phylogenetic evidence of host-specific cryptic species in the anther smut fungus. *Evolution*, **61**(1): 15–26. doi:10.1111/j.1558-5646.2007.00002.x. PMID:17300424.
- Lutz, M., Göker, M., Piatek, M., Kemler, M., Begerow, D., and Oberwinkler, F. 2005. Anther smuts of Caryophyllaceae: molecular characters indicate host-dependent species delimitation. *Mycol. Prog.* **4**(3): 225–238. doi:10.1007/s11557-006-0126-4.
- Lutz, M., Piatek, M., Kemler, M., Chlebicki, A., and Oberwinkler, F. 2008. Anther smuts of Caryophyllaceae: molecular analyses reveal further new species. *Mycol. Res.* **112**(Pt 11): 1280–1296. doi:10.1016/j.mycres.2008.04.010. PMID:18951773.
- McDowell, E.M., and Trump, B.F. 1976. Histologic fixatives suitable for diagnostic light and electron microscopy. *Arch. Pathol. Lab. Med.* **100**(8): 405–414. PMID:60092.
- Mendgen, K., Hahn, M., and Deising, H. 1996. Morphogenesis and mechanisms of penetration by plant pathogenic fungi. *Annu. Rev. Phytopathol.* **34**(1): 367–386. doi:10.1146/annurev.phyto.34.1.367. PMID:15012548.
- Mercier, J., and Lindow, S.E. 2000. Role of leaf surface sugars in colonization of plants by bacterial epiphytes. *Appl. Environ. Microbiol.* **66**(1): 369–374. doi:10.1128/AEM.66.1.369-374.2000. PMID:10618250.
- Poon, N.H., Martin, J., and Day, A.W. 1974. Conjugation in *Ustilago violacea*. I. Morphology. *Can. J. Microbiol.* **20**(2): 187–191. doi:10.1139/m74-029. PMID:4822787.
- Refrégier, G., Le Gac, M., Jabbour, F., Widmer, A., Shykoff, J.A., Yockteng, R., Hood, M.E., and Giraud, T. 2008. Cophylogeny of the anther smut fungi and their caryophyllaceous hosts: prevalence of host shifts and importance of delimiting parasite species for inferring cospeciation. *BMC Evol. Biol.* **8**(1): 100 [online]. doi:10.1186/1471-2148-8-100. PMID:18371215.
- Shykoff, J.A., Bucheli, E., and Kaltz, O. 1996. Flower lifespan and disease risk. *Nature*, **379**(6568): 779. doi:10.1038/379779a0.
- Snetselaar, K.M., and Mims, C.W. 1992. Sporidial fusion and infection of maize seedlings by the smut fungus *Ustilago maydis*. *Mycologia*, **84**(2): 193–203. doi:10.2307/3760250.
- Snetselaar, K.M., and Mims, C.W. 1993. Infection of maize stigmas by *Ustilago maydis*: light and electron microscopy. *Phytopathology*, **83**(8): 843–850. doi:10.1094/Phyto-83-843.
- Uchida, W., Matsunaga, S., Sugiyama, R., Kazama, Y., and Kawano, S. 2003. Morphological development of anthers induced by the dimorphic smut fungus *Microbotryum violaceum* in female flowers of the dioecious plant *Silene latifolia*. *Planta*, **218**(2): 240–248. doi:10.1007/s00425-003-1110-8. PMID:14551772.
- Uchida, W., Matsunaga, S., and Kawano, S. 2005. Ultrastructural analysis of the behavior of the dimorphic fungus *Microbotryum violaceum* in fungus-induced anthers of female *Silene latifolia* flowers. *Protoplasma*, **226**(3-4): 207–216. doi:10.1007/s00709-005-0113-7. PMID:16333578.
- Vánky, K. 1994. *European smut fungi.* Gustav Fischer, Stuttgart, Jena, New York, N.Y.
- Weiss, M., Bauer, R., and Begerow, D. 2004. Spotlights on heterobasidiomycetes. In *Frontiers in basidiomycote biology.* Edited by R. Agerer, M. Piepenbring, and P. Blanz. IHW-Verlag, Echtingen, Germany. pp. 7–48.

- Werth, E. 1911. Zur biologie des Antherenbrandes. Arbeiten aus der Kaiserlichen Biologischen Anstalt für Land- und Forstwirtschaft, **8**(3): 427–450.
- Witt, T., Jürgens, A., Geyer, R., and Gottsberger, G. 1999. Nectar dynamics and sugar composition in flowers of *Silene* and *Saponaria* species (Caryophyllaceae). Plant Biol. **1**(3): 334–345. doi:10.1111/j.1438-8677.1999.tb00261.x.
- Yockteng, R., Marthey, S., Chiapello, H., Gendrault, A., Hood, M.E., Rodolphe, F., Devier, B., Wincker, P., Dossat, C., and Giraud, T. 2007. Expressed sequences tags of the anther smut fungus, *Microbotryum violaceum*, identify mating and pathogenicity genes[online]. BMC Genomics, **8**(1): 272. doi:10.1186/1471-2164-8-272. PMID:17692127.